TECHNICAL ARTICLE

Phase Evolution at the Interface between Liquid Solder Sn-Zn-Ag and Cu Substrate Studied by In Situ Heating Scanning Transmission Electron Microscopy

Paweł Czaja, Aleksandra Dybeł, and Janusz Pstruś

Wetting phenomena concerning Sn-Zn eutectic alloys with Ag addition were studied in contact with Cu substrate at 250 °C and in the presence of ALU33 flux. The chosen wetting time was 5 s. Then in situ STEM isothermal heating at 150 °C lasting for 10, 40 and 70 min was conducted to establish the sequence of phase appearance. The intermetallic phases within the Cu-Zn system were identified. The formation sequence and interface microstructure were determined. It is demonstrated that the ε-Cu(Ag)Zn$_4$ phase appears first and it is followed by the γ-Cu(Ag)$_5$Zn$_8$. The resulting Cu saturated solder transforms into γ phase taking scallop-like shape.

1. Introduction

The Sn-Zn eutectic alloy with melting point of 198.6 °C is a promising alternative to conventional Sn-Pb eutectic solder (183 °C) that needs to be replaced due to modern environmental regulations and policies. And although in general it compares favorably, especially in terms of melting point, components abundance and cost efficiency, the primary limitations, which prohibit the more widespread use of Sn-Zn eutectic solder in packaging and electronic industry, arise from its poor wettability (Ref 1). The latter is owed on the one hand to the insufficient oxidation resistance, compromised by highly active Zn element, and on the other to large surface tension dictated by a considerable quantity of Zn (Ref 2). Hence, in order to overcome these limitations and improve wettability the Sn-Zn eutectic solder system is alloyed with trace amounts of different elements including Ag, which has been shown to enhance oxidation resistance of Sn-Zn solder (Ref 3, 4, 5]. It has been found (Ref 6) that with increasing Ag content in the solder system the Zn oxide layer on the surface becomes reduced. This is related to the appearance of intermetallic

phases within the Ag-Zn system. The amount of Ag required needs to be above 0.5 wt.% since only above this level the Ag and Zn are prone to interact and produce Ag-Zn IMCs (Ref. 7). Chen et al. (Ref 8) studied microstructure of the interface between the Sn$_9$Zn$_1$Ag (wt.%.) and a Cu substrate. They have found that after the wetting test there is only 0.3 wt.% of Ag left in the solder alloy, while at the interface there appear IMCs from within the Cu-Zn and Ag-Zn systems. These phases are unfortunately detrimental for the mechanical properties of solder joint.

Nonetheless simultaneously the increase in Ag content elevates the onset melting temperature and narrows the melting temperature range in the Sn-Zn solder system (Ref 9). For instance, in comparison between the Sn-9Zn solder system containing 1 wt.% addition of Ag with a Ag-free solder, the melting temperature range will go down by 56.2% (Ref 3), what in result enhances viscosity of the solder. In terms of mechanical properties, the Ag addition has also been found to increase the pull force at the solder/Cu joints depending on the Ag content. When the amount of Ag is around 1 wt. % the pull force is near the value for the primary Sn-9Zn. With respect to creep behavior, Ag doping into Sn-Zn eutectic alloy is reported to enhance creep resistance due to the pinning action for moving dislocations from AgZn and Ag$_3$Sn intermetallic phases. Interestingly the introduction of Ag alters the microstructure. It has been noted that with 1.5 wt.% addition of Ag the morphology of Zn-rich phases evolves from needle-like to rod-like. Moreover, new Ag-Zn phases have been recognized, i.e., AgZn, γ-Ag$_5$Zn$_8$ and ε-AgZn$_3$. These new phases typically are finely distributed, what promotes increased ultimate tensile strength and ductility (Ref 10, 11).

Regardless of the composition, the primary consideration for a mechanically stable solder/substrate interface is an interfacial layer. It results from a series a of phenomena entailing wetting, spreading, filling of the gaps and eventually producing a metallurgical bonding. The bonding itself is determined by dissolution, diffusion and solidification processes. While the mechanism itself can be quite complex (Ref 12), the resulting

Paweł Czaja, Aleksandra Dybeł, and **Janusz Pstruś**, Institute of Metallurgy and Materials Science, Polish Academy of Sciences, Reymonta Street 25, 30-059 Krakow, Poland. Contact e-mail: p.czaja@imim.pl.

microstructure determines the resultant mechanical properties of the joint. Typically, such a microstructure is made up of a number of intermetallic phases appearing in a close proximity to the solder/substrate interface. There are certain microstructural requirements for the intermetallic phases; e.g., they cannot be too thick (adverse effect of reliability of the solder joint) neither too thin (poor metallurgical bond); ideally their thickness resides in a desired range specified by the system in question. Hence the interfacial microstructure plays a pivotal role in determining the strength and stability of the solder joints (Ref 13, 14). In this contribution we have thus studied the interfacial phase evolution in the Sn-Zn-Ag solder contacting the Cu substrate by in situ scanning transmission electron microscopy (STEM), which allowed for pin pointing the subtle microstructural and chemical composition changes in microareas near the interface while thin foil heating.

2. Experimental

Solder for tests was prepared by melting pure metals (Sn: 99.999, Zn: 99.95, and Ag: 99.999%) in adequate proportions in graphite crucibles, in a glovebox filled with Ar (99.9992%) protective atmosphere (oxygen and water vapor pressure less than 1 ppm) to avoid oxidation. Wetting tests were carried out using the sessile drop (SD) method at 250 °C for 5 s. Experimental setup allows for rapid sample transfer to and from the oven heat zone, allowing for precise hold time control (Ref 15). The weight of each sample used for wetting tests was 0.5 g, and the dimensions of the copper washers were 30×30 mm. The copper washers were prepared in accordance with EN ISO 9455–10:2000. Wetting tests were conducted using ALU33 flux that was applied to both solder and the copper substrate. Selected solidified solder pairs/substrate were cut perpendicular to the interface plane, mounted in conductive resin and polished to characterize the microstructure by scanning electron microscopy (SEM) combined with energy-dispersive x-ray spectroscopy (EDS). A conductive carbon coating was sputtered onto the surface of the samples to protect against oxidation. Thin foils for STEM were prepared by focused ion beam (FIB) technique using Thermo-Scientific SCIOS 2 DualBeam. The microscope used was Thermo-Scientific Titan Themis x-FEG G3 Cs-corrected S/TEM. The in situ investigations were conducted on the FEI's NanoExTM-i/v TEM single-tilt heating/biasing holder based on a consumable semiconductor MEMS device as the heater. This holder has much advantage over more conventional TEM heating holders in terms of precise and speedy heat delivery. It affords also substantially reduced thermal drift due to low thermal mass. The overview of a typical holder grid is shown in Fig. 1(a). The schematic of thin lamella mounted over one of the hollow grids is presented for illustration in Fig. 1(b). In situ heat treatment was performed at 150 °C for various times, i.e., 10, 40 and 70 min. After each isothermal step the lamellae was cooled down to ambient temperature for inspection and analysis.

3. Results and Discussion

A typical microstructure of a cross section of the Sn-Zn-Ag eutectic solder alloys is presented in Fig. 2(a). According to the scanning electron microscopy backscatter electron (BSE) contrast, the microstructure is composed of three phases distinguished by contrast difference: light grey corresponding to the matrix β-Sn; dark eutectic needles of α-Zn phase, while the darkest contrast grains correspond to AgZn₃. The phases appear to be non-uniformly distributed. The large areas with weak grey contrast are associated with Zn-free zones. The Zn-rich phase takes form of a rod-like precipitates distributed throughout the sample surface. It coexists with round-like precipitates with dark contrast. The EDS analysis confirmed the phase composition. The bright grey contrast phase is primarily Sn with trace amounts of Zn at the level around 1 at.%. The rod-like phase (Fig. 3) is made up of α-Zn. Whereas the darkest contrast phase, which appears in the smallest volume contribution, is rich in Zn and is made up of 76.9 at. % Zn, 20.2 at. % Ag, a small amount of Cu (2.2 at. %) and a trace amount of Sn (0.3 at. %) are noted. During the test, copper diffuses from the substrate and is fully dissolved in the AgZn3 phase where it replaces the Ag atoms. The Ag-Zn intermetallic compounds are observed in the Sn-Zn-Ag solders when the concentration of Ag exceeds 0.5% by weight (Ref 16). These differences in phase composition are well illustrated in the BSE image provided with the corresponding elemental distribution maps in Fig. 3. In consistence with the EDS point analysis, the matrix is made up of a Sn-rich phase, while the precipitates are Zn-Ag intermetallics. These results are largely consistent with the literature (Ref 17).

Figure 2b shows a cross section of the SnZnAg/Cu solder joint after 5 s of heating at $T = 250$ °C. One can see that at the solder/substrate interface, a transition layer is formed consisting of two intermetallic phases: on the Cu side, a thin phase consisting of Zn and Cu is formed, and on the solder side, a shell-like phase consisting mainly of Zn and Ag is developed. A close-up image on the solder/substrate interface is shown in Fig. 2(b). It can be seen that the microstructure of the interface bears a scallop-like features. The chemical composition evolves across the solid/substrate interface. It can be well traced with a line scan analysis (Fig. 4). Figure 4(a) shows a secondary electron (SE) image with a line scan distance marked by the arrow. The line scan results are portrayed in Fig. 4(b). From the results (Fig. 4(b)) it is easily observable how Sn, the main constituent of the solder, is gradually replaced by the Zn-Ag intermetallic phase as the line scan approaches the substrate layer. Some earlier works concerning interactions between Sn-Zn-Ag solders and a Cu substrate (Ref 6-8, 18) have reported that the interface is composed of the continuous γ-Cu₅Zn₈ phase and large grains of AgZn₃. These grains grow together with increasing Ag content what worsens the mechanical properties of the joint. However the reflow time in (Ref 6-8, 18) was much longer (several minutes) than in the present study.

A more detailed investigation of the interface was conducted by TEM. Figure 5(a, b) shows bright field (BF) images, while
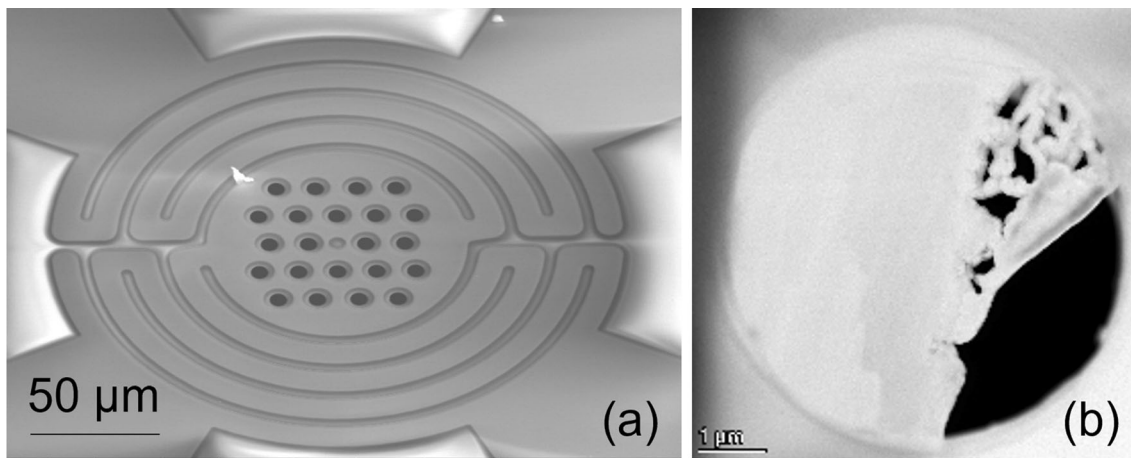
Fig. 1 An overview of the MEMS-based chip for lamella mounting (a); an illustrative image of a thin lamella mounted over one of the hollow grids (b)
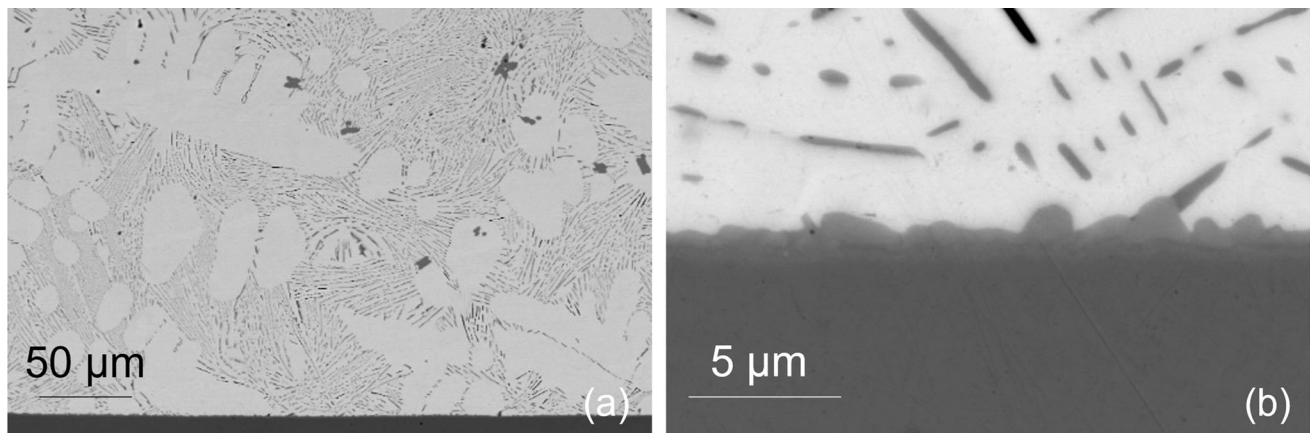

Fig. 2 Backscatter electron microscopy images of the cross-sectioned bulk Sn-Zn-Ag eutectic solder alloy; a bird view (a) and a close-up on the solder/substrate interface (b)

Fig. 5(c) shows an example STEM-HAADF image taken from the thin lamellae cut out from the cross section along the direction perpendicular to the interface (similar to the position or the arrow in Fig. 4(a). The outer parts of the lamella (Fig. 5a) represent the solder (left-hand side) and the Cu substrate (right-hand side), whereas the middle of the image is taken up by the interface. The microstructure appears quite complex. It can be better resolved on the magnified BF image (Fig. 5b) and on the STEM-HAADF image (Fig. 5c), where distinct phase can be told apart.

In Fig. 6, one can find a magnified STEM-HAADF image (a) presented together with the corresponding STEM-EDS element distribution map (b). These results are well consistent with earlier SEM–EDX analysis (Fig. 3, Fig. 4). According to the measured composition it was possible to identify different phases. By observing the areas occupied by distinct phase it is possible to infer the sequence of the phase appearance. The phases are well confirmed by selected area electron diffraction patterns (SADPs) taken from the interface region and given together with the respective BF images (Fig. 7).

It can be assumed that in the first stage of the Cu substrate wetting process with the (SnZn)eut. + 1%Ag solder, Zn atoms diffuse to the copper surface, dissolving the substrate. As a result of this process, Cu atoms diffuse into the liquid, what

produces a reaction zone (RZ) (Ref 9). Over time, this zone is saturated with both Cu and Zn atoms. Under typical circumstances in the reaction of the Sn-Zn solder with the Cu substrate, the first to appear is the ε phase and subsequently in result of counter diffusion of Cu into the solder the γ phase appears. In the present scenario however, in the reaction of the ternary Sn-Zn-Ag solder with the Cu substrate the ε-AgZn$_3$ phase is already pre-existing in the solder (Fig. 2a and Fig. 3). The formation of the epsilon phase in the solder consumes zinc, what then leads to Zn depletion within the solder. Therefore, the RZ formed with the SnZnAg solder is more slowly saturated with Zn than that with the SnZn solder, and the γ-Cu$_5$Zn$_8$ phase crystallizes in the interface. After melting the solder at a temperature of 250 °C, the AgZn$_3$ grains are dissolved by the liquid and, as a result, they disintegrate into small nanograins. The epsilon phase nanograins migrate to the interface where they coagulate on the formed gamma phase (Fig. 6b). The different migration speed results in the formation of a scallop microstructure. In order to corroborate these deductions an in situ STEM isothermal heating experiment was performed on a freshly cut lamella. The results are shown in Fig. 8, which shows the STEM-HAADF image with the corresponding element distribution map (bottom) taken from the lamella prior to heating experiment. According to the composition measured
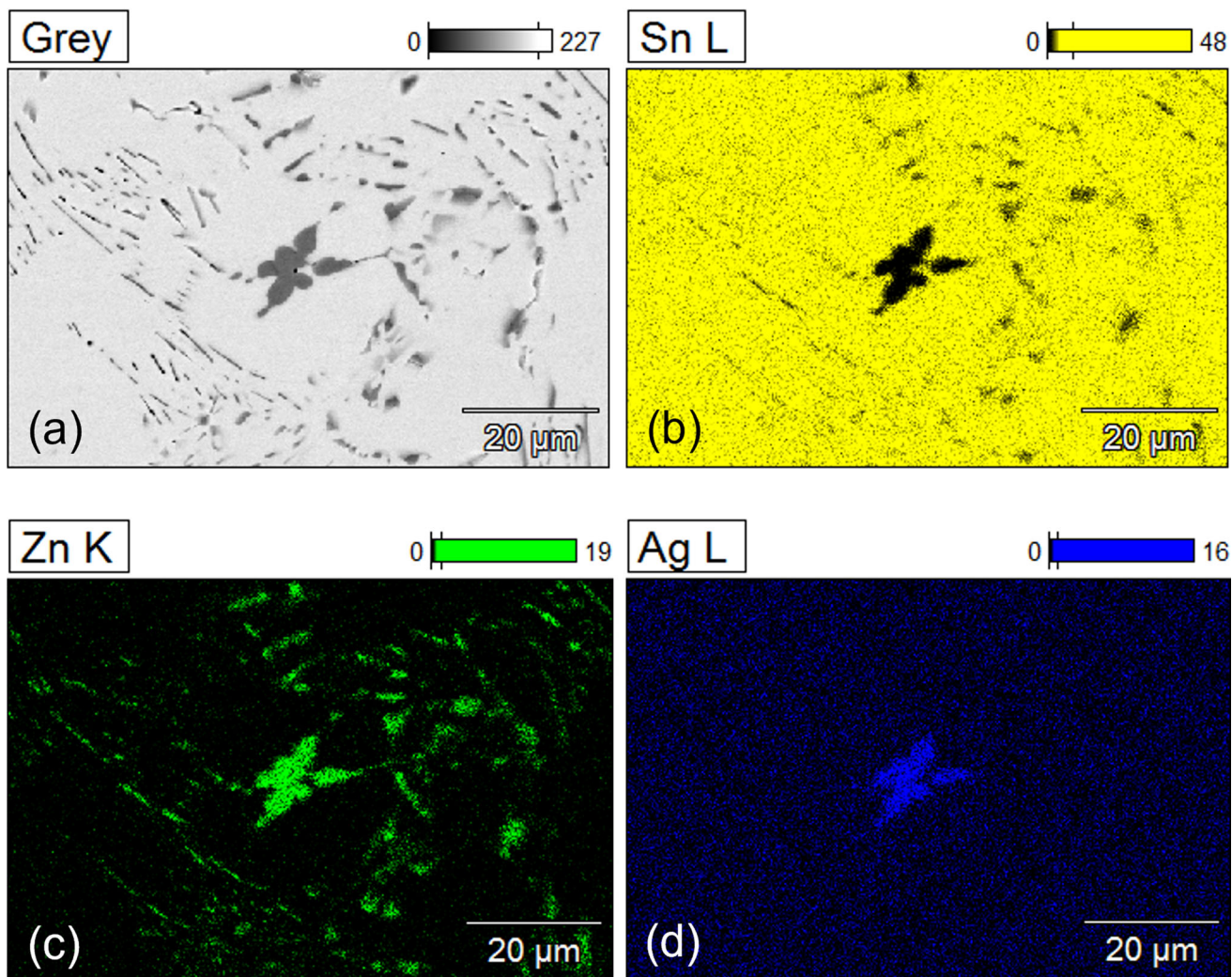
Fig. 3 Backscatter electron image (a) and the corresponding element distribution maps of Sn (b), Zn (c) and Ag (d) taken from the cross section of the cast Sn-Zn-Ag eutectic solder
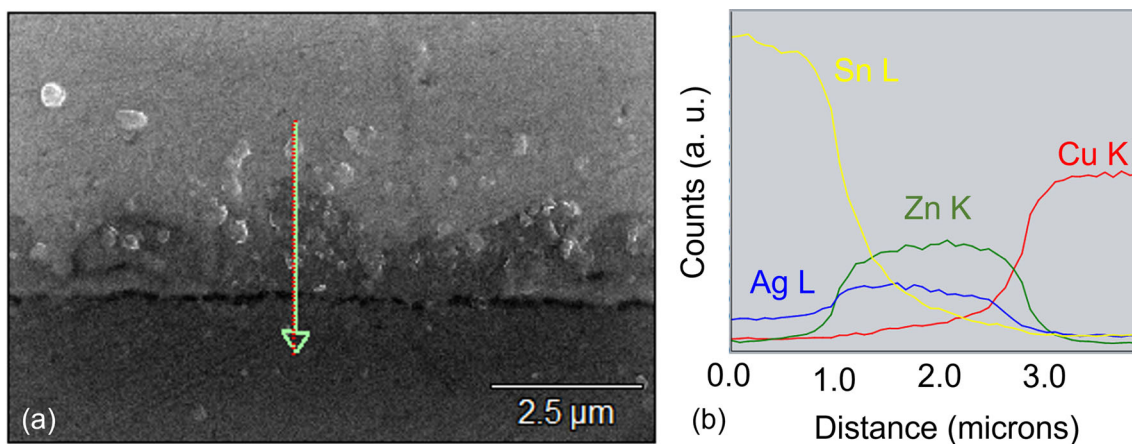
Fig. 4 Line scan analysis across the solder/substrate interface imposed on the secondary electron image (a) together with the EDS counts as a function of distance in μm (b)
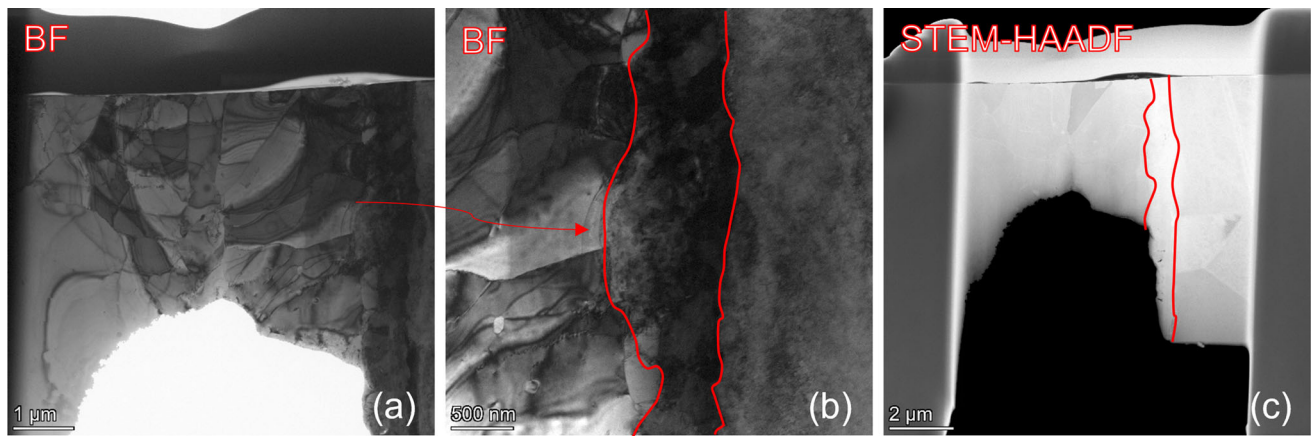
Fig. 5 Bright field (a, b) and the STEM-HAADF (c) images of the thin lamella cut out from the solid/substrate interface in the Sn-Zn-Ag eutectic solder
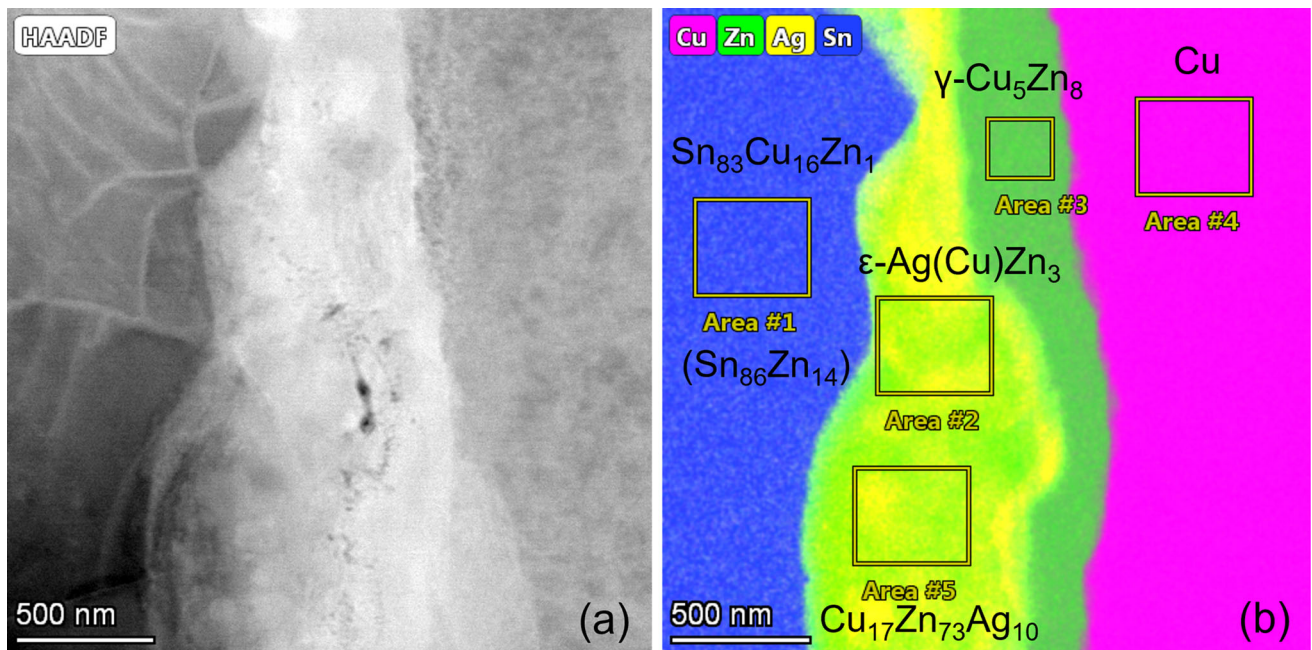

Fig. 6 STEM-HAADF image of the interface (a) and the corresponding element distribution map (b) taken from the thin lamellae Sn-Zn-Ag eutectic solder

it was possible to identify individual phases, which are named on the image. Then in situ heating was performed by elevating the temperature to 150 °C and isothermally keeping the lamellae at this temperature for 10 min Fig. 8(b), 40 min (c) and 70 min (d).

Figure 8 (a) shows the initial state of the interface prior to heating at 150 °C. One can note the disappearance of the ε – phase observed in Fig. 6b. This is most likely due to heating incurred by the thin lamella preparation. For the heating experiment, a second lamella was cut out and it had to be much thinner than the initial one (Fig. 6) what meant longer exposure to Ga^+ ion beam and a thinner volume. In addition the lamella had to be transferred and welded by Pt onto a special MEMS-based heating holder (Fig. 1), what introduced additional local heating step, while sample preparation. Thus, Fig. 8(a) is taken as the starting point for the in situ experiment.

From the image (Fig. 8) one can note a considerable microstructural changes entailing the formation of voids and pores (top row) as well as substantial chemical composition evolution (bottom row) in result of diffusion process as the time on isothermal annealing is extended. In this scenario, an initial aging of the interface is observed. In the solder, there was a drastic depletion of Zn. On the one hand it is related to the participation of Zn assisting in the formation of interfacial intermetallic phases and on the other hand, to a very small sample size. The very small size prevented the inflow of
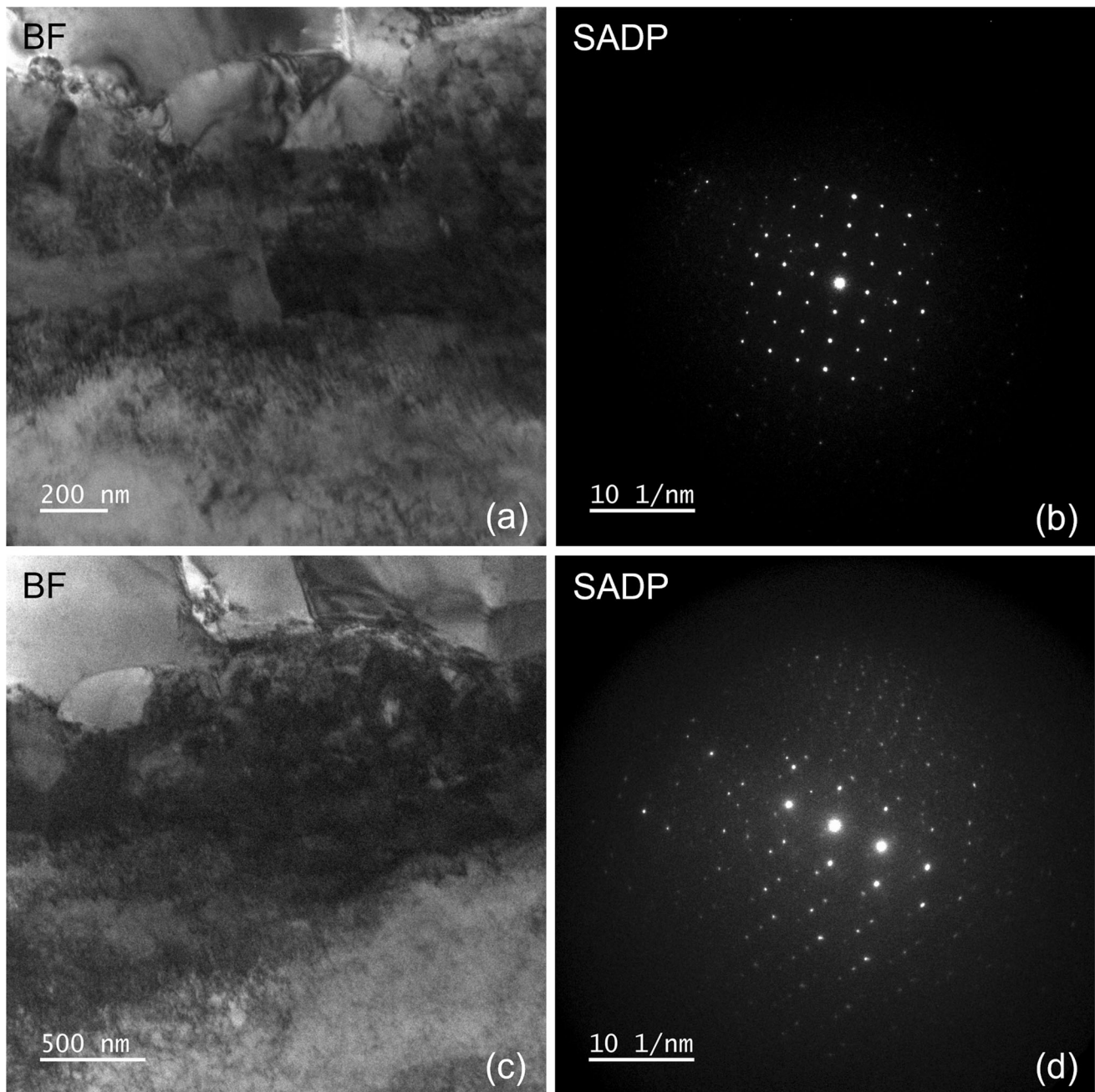
Fig. 7 Bright field images (a, c) and the corresponding selected electron diffraction patterns (b, d) taken from the thin lamellae Sn-Zn-Ag eutectic solder

"fresh" Zn atoms from the solder, and on the other hand, we were constantly dealing with the diffusion of Cu atoms from the substrate. In the absence of free Zn atoms, the η-Cu_6Sn phase was formed in the solder, and the scallop ε-$Ag(Cu)Zn_3$ phase, after reacting with Cu atoms, was transformed into the γ-$Cu(Ag)_5Zn_8$ phase. During the aging process, RZ was constantly saturated with Cu atoms from the substrate and Sn atoms from the solder. As a result of these processes, the originally existing intermetallic phases (Fig. 6) were transformed from the high zinc (gamma and epsilon) to the high copper beta phase. Moreover, the Sn atoms diffusing into the IMCs layer started the process of its dissolution. The destruction of this layer can lead to a significant deterioration of the properties of the solder joint.

4. Conclusions

In situ experiments demonstrated the sequence of interfacial phase evolution during heating. Lower free energy of Zn favors phase formation from the Cu-Zn over Cu-Sn system. First to appear is the ε-$Cu(Ag)Zn_4$ phase. Subsequent counter diffusion of Cu and Zn stimulates the formation of γ-$(Ag)_5Zn_8$. The Cu element diffuses through the intermetallic layer resulting in solder saturation. Saturated solder transforms into γ phase resulting in scallop growth. Growing scallops detach and migrate into the solder. Long annealing results quite likely in β-phase formation.
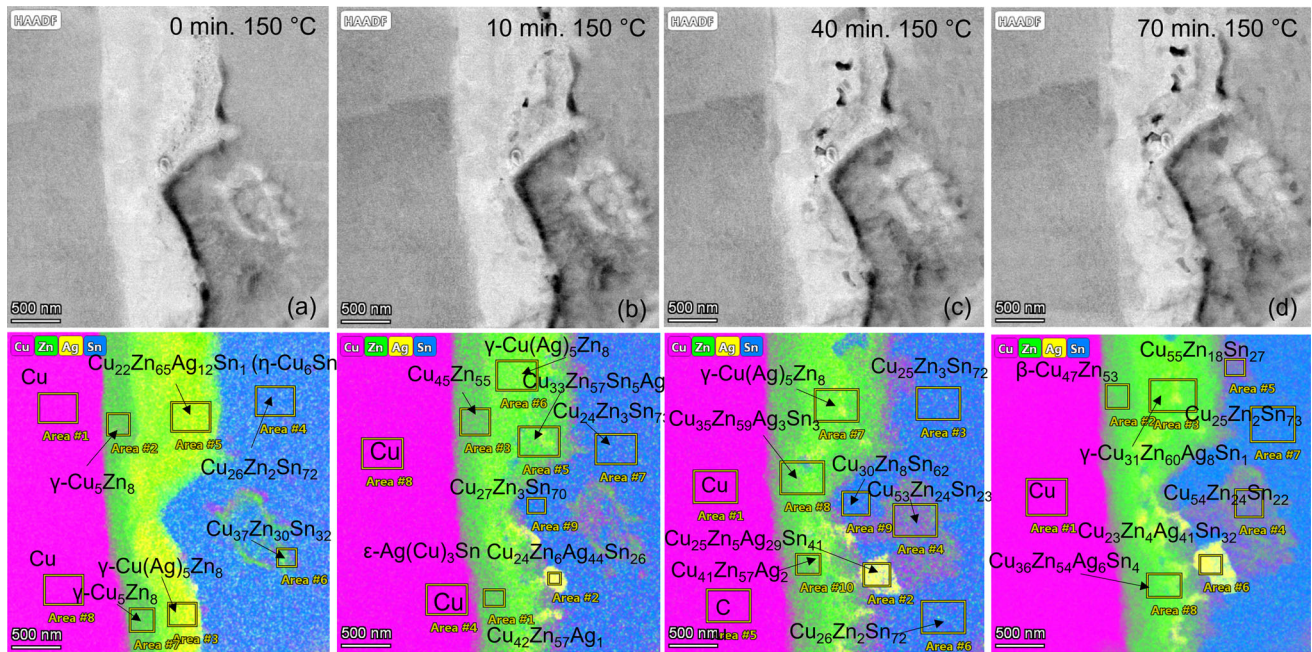
Fig. 8 STEM-HAADF (a-d) and the corresponding element distribution maps taken from the thin lamellae of the Sn-Zn-Ag eutectic solder following isothermal heat treatment steps 0, (a), 10 (b), 40 (c) and 70 min (d)

References

1. S. Liu, S. Xue, and P. Xue, Present Status of Sn-Zn lead-Free Solders Bearing Alloying Elements, *J. Mater. Sci.: Mater Electron.*, 2015, **26**, p 4389–4411

2. C. Morando, O. Fornaro, O. Garberllini et al., Thermal Properties Od Sn-Based Solder Alloys, *J. Mater. Sci. Mater. Electron.*, 2014, **25**(8), p 3440–3447

3. K.L. Lin and C.L. Shih, Microstructure and Thermal Behavior of Sn-Zn-Ag Solders, *J. Electron. Mater.*, 2003, **32**(12), p 1496–1500

4. S.W. Park, S. Nago, T. Sugahara et al., Retarding Intermetallic Compounds Growth of Zn High-Temperature Solder and Cu Substrate by Trace Element Addition, *J. Mater. Sci. Mater. Electron.*, 2013, **24**(12), p 4704–4712

5. F. Li, C. Pu, C. Li et al., Study on the Effects of Ag Addition on the Mechanical Properties and Oxidation Resistance of Sn–Zn Lead-Free Solder Alloy by High-Throughput Method, *J Mater Sci: Mater Electron*, 2023, **34**, p 322. https://doi.org/10.1007/s10854-022-09756-8)

6. T.K. Yeh, K.L. Lin, and B. Salam, Improving High-Temperature Oxidation Behaviour of Sn-Zn-Ag-Al-Ga Solders, *Solder. Surf. Mt. Tech.*, 2009, **21**, p 19–23

7. Y.H. Hu, S.B. Xue, W.X. Chen et al., Investigation on the Wettability and Interfacial Structure of Sn-9Zn-xAg Solders on Cu Substrate, *J Mater Eng*, 2009, **16**, p 60–63

8. W.X. Chen, S.B. Xue, H. Wang, J.X. Wang, Z.J. Han, and L.L. Gao, Effects of Ag on Microstructures, Wettabilities of Sn–9Zn–xAg Solders as well as Mechanical Properties of Soldered Joints, *J Mater Sci: Mater Electron*, 2010, **21**, p 461–467. https://doi.org/10.1007/s10854-009-9939-7

9. F.Y. Hung, C.J. Wang, S.M. Huang et al., Thermoelectric Characteristics and Tensile Properties of Sn–9Zn–xAg Lead-Free Solders, *J. Alloy. Compd.*, 2006, **420**(1), p 193–198

10. W. Chen, S. Xue, H. Wang et al., Effects of Ag on Properties of Sn-9Zn Lead-Free Solder, *Rare Met. Eng.*, 2010, **39**(10), p 1702–1706

11. M.L. Huang, X.L. Hou, N. Kang et al., Microstructure and Interfacial Reaction of Sn-Zn-x (Al, Ag) Near-Eutectic Solders on Al and Cu Substrates, *J. Mater. Sci. Mater. Electron.*, 2014, **25**(5), p 2311–2319

12. J. Pstruś, *J. Mater. Sci.: Mater. Electron.*, 2018, **29**, p 20531–20545. https://doi.org/10.1007/s10854-018-0197-4

13. J.W. Yoon and S.B. Jung, Reliability Studies of Sn-9Zn/Cu Solder Joints with Aging Treatment, *J. Alloys. Compd.*, 2006, **407**(1), p 141–149

14. T. Gancarz, P. Fima, and J. Pstruś, Thermal Expansion, Electrical Resistivity, and Spreading Area of Sn-Zn-In Alloys, *J. Mater. Eng. Perform.*, 2014, **23**(5), p 1524–1529

15. J. Pstruś, P. Fima, and T. Gancarz, Wetting of Cu and Al by Sn-Zn and Zn-Al Eutectic Alloys, *J. Mater. Eng. Perform.*, 2012, **5**(21), p 606–613

16. K.L. Lin and C.L. Shih, Microstructure and Thermal Behaviour of Sn-Zn-Ag Solders, *J. Electron. Mater.*, 2003, **32**(12), p 1496–1500

17. A.A. El-Daly and A.E. Hammad, Effects of Small Addition of Ag and/or Cu on the Microstructure and Properties of Sn-9Zn Lead-Free Solders, *Mater. Sci. Eng. A*, 2010, **527**(20), p 5212–5219

18. H. Wang and Sb. Xue, Effect of Ag on the Properties of Solders and Brazing Filler Metals, *J Mater Sci: Mater Electron*, 2016, **27**, p 1–13

Publisher's Note Springer Nature remains neutral with regard to jurisdictional claims in published maps and institutional affiliations.